Post-print of: Lentka Ł., Kotarski M., Smulko J., Cindemir U., Topalian Z., Granqvist C., Calavia R., Ionescu R.: Fluctuation-Enhanced Sensing with Organically Functionalized Gold Nanoparticle Gas Sensors Targeting Biomedical Applications. TALANTA. Vol. 160 (2016), pp.9-14. DOI: 10.1016/j.talanta.2016.06.063

Fluctuation-Enhanced Sensing with Organically Functionalized Gold Nanoparticle Gas Sensors Targeting Biomedical Applications

Łukasz Lentka[1], Mateusz Kotarski[1], Janusz Smulko[1], Umut Cindemir[2], Zareh Topalian[2], Claes G. Granqvist[2], Raul Calavia[3], Radu Ionescu[3]

[1]Faculty of Electronics, Telecommunications and Informatics, Gdansk University of Technology, Narutowicza 11/12, 80-233 Gdansk, Poland

[2]Department of Engineering Sciences, The Ångström Laboratory, Uppsala University, SE-75121 Uppsala, Sweden

[3]Department of Electronics, Rovira i Virgily University, 43006 Tarragona, Spain

Corresponding Authors

Janusz Smulko: Tel.: +48-58-348-6095; Fax: +48-58-348-6373 jsmulko@eti.pg.gda.pl

Radu Ionescu: Tel.: +34-977-55-8764; Fax: +34-977-55-9605 radu.ionescu@urv.cat

ABSTRACT

Detection of volatile organic compounds is a useful approach to non-invasive diagnosis of diseases through breath analysis. Our experimental study presents a newly developed prototype gas sensor, based on organically-functionalized gold nanoparticles, and results on formaldehyde detection using fluctuation-enhanced gas sensing. Formaldehyde was easily detected via intense fluctuations of the gas sensor's resistance, while the cross-influence of ethanol vapor (a confounding factor in exhaled breath, related to alcohol consumption) was negligible.

Keywords

Organically-functionalized gold nanoparticles, formaldehyde detection, fluctuation enhanced sensing, flicker noise

1. Introduction

Numerous volatile organic compounds (VOCs) are produced inside the human body as a consequence of metabolic processes and the lighter blood-soluble VOCs (mainly nonpolar compounds) exchange in the alveoli and are released to the exterior through exhaled breath [1]. When a disease is onset, some VOCs are released in concentrations that are different from those in the normal state, and new VOCs can be also produced and utilized for non-invasive detection of the disease through exhaled breath analysis [1, 2]. Formaldehyde is an interesting VOC for such biomedical applications and has been identified as a potential cancer biomarker in exhaled breath [3-5].

In medical applications targeting high-risk populations, screening for early diagnosis of a disease—which may then be easy to treat—by VOC detection requires cheap vapor

sensors that are highly sensitive to the VOCs of interest and also tolerant for confounding compounds (*e.g.*, ethanol vapor related to alcohol consumption). Sensors based on monolayer-capped gold nanoparticle (AuNP) films are of much interest and offer several advantages such as low detection limits for nonpolar VOCs, room temperature operation, small dimensions, and low cost [6]. These sensors' sensitivity and selectivity can be tailored by proper selection of their organic functionality, which provides the chemical sensing, while the gold nanoparticles produce electrical conduction through the film. Such sensors can be produced by use of various technologies and exhibit high sensitivity to selected gases—even to a group of the VOCs of present interest [3]. An overview of such gas sensors, based on gold nanoparticles doped with selected dopants (e.g., TiO_2, WO_3) and prepared by various technologies, can be found elsewhere [7–9]. The emerging technologies can be developed rapidly and they can be optimized with regard to cost, improved selectivity and way of gas sensing via DC resistance or the presented fluctuation-enhanced gas sensing.

Adsorption–desorption phenomena involving the sensing material and the sensed VOCs may result in changes of the gas sensor's electrical properties, such as its DC resistance [10] and/or resistance fluctuations [11, 12]. Resistance fluctuations are expected to show the highest sensitivity to changes in the ambient atmosphere, because one can expect lower energy expenditure in order to induce fluctuations than to change the DC resistance, and consequently fluctuation-enhanced sensing can be extended to lower gas concentrations than DC-resistance-based sensing [13]. Moreover, DC resistance provides a single parameter whereas resistance fluctuations can be characterized, typically, by a power spectral density (PSD) which is a function of frequency and therefore gives more information than a single parameter value.

2. Material and methods

Conventional AuNP synthesis is based on a wet-chemistry method developed by Brust *et al*. [14] and makes use of precursors and reagents. This method leaves traces of residual compounds attached to the AuNPs even after the application of purification processes [15], and this contamination may affect the properties of the sensing film. In the present work, we produced AuNPs by an innovative method that employs the Advanced Gas Deposition (AGD) technique [16]. Our methodology for sensor preparation comprises two steps and ensures the fabrication of ultra-pure monolayer-capped gold nanoparticles. AuNPs were first deposited by AGD onto specially designed sensing substrates so as to cover a region with a 30-μm-wide and 1.3-mm-long gap between gold electrodes (see Supporting Information) as shown in Figure 1a. To this end, a high-purity piece of gold (99.999%) was placed inside an induction coil in the evaporation chamber of the AGD unit and was heated to a temperature exceeding the melting point of gold so that Au atoms were evaporated. A laminar flow of an inert gas (He at a flow rate of 20 l/min) with upward direction transported the AuNPs that had nucleated and grown in the gas through a transfer pipe (3 mm inner diameter) to the deposition chamber of the AGD unit where the sensor substrate was positioned. The AuNPs became attached to the sensor substrate and formed a dispersed monolayer.

The sensor substrate with deposited AuNPs was then immersed for 1 h in a solution of 150 mg of 2-mercaptobenzoxazole (C_7H_5NOS) dissolved in 20 ml of ethanol, and the sensor was finally dried at 50 ºC for 1 h in a conventional oven in order to remove the organic solvent. This dip-coating process produced a monolayer of ~10-nm-diameter AuNPs capped with organic ligands, as shown by scanning electron microscopy (SEM) in Figure 1b. The elemental composition of the sensor's surface was probed by x-ray photoemission spectroscopy (XPS), which showed nothing but the presence of Au from

the AuNPs, elements from the organic compound (C, O and N), and Si and O from the substrate owing to its incomplete coverage by the AuNP-based layer (Figure 1c).

3. Results and Discussion

The sensors exhibited nonlinear current–voltage characteristics resembling a Schottky diode behavior (Figure 2). Electron-beam-induced current (EBIC) analysis (see Supplementary Material), performed with the scanning electron microscope, showed the formation of depletion layers between the metallic gold electrodes and the *p*-type semiconducting material comprising the gas sensor, thus indicating that the Schottky effect is produced between these components of the device.

Gas sensing experiments were conducted by placing the AuNP-based sensor inside a one-liter test chamber and exposing it during 20-minute cycles to different vapors at a flow rate that was sufficiently low (50 ml/min) to avoid turbulence. A constant bias voltage U_B was applied between the sensor's electrodes. The gases were pure synthetic air (SA; 20% oxygen and 80% nitrogen), SA with ~1.5 ppm of formaldehyde (HCHO), and SA with 50 ppm of ethanol (C_2H_5OH). Formaldehyde vapor was generated from formalin, *i.e.*, a commercial solution of 30% formaldehyde in water. A data acquisition system measured the DC voltage across the sensor and its fluctuations (resistance noise) using a high-precision data acquisition board (NI PCI-4474) without additional amplification.

There was no noticeable difference in the gas sensor's DC characteristics when the ambient atmosphere was changed from pure SA to SA with formaldehyde or ethanol. However, the application of a high bias voltage (U_B = 11.3 V) led to the generation of intense fluctuations (short spike-pulses) with amplitudes of tens of mV (Figure 3a). These fluctuations were observed at a sampling frequency of 100 kHz. In order to estimate the

PSD, we recorded 8×2^{10} consecutive noise samples in each experimental run and averaged over 1000 spectra to reduce the random error to as little as 3% [17]. The same noise samples were used to estimate the probability distribution of the recorded noise amplitudes as a histogram. The random error of the calculated histogram did not exceed a few percent for the largest noise amplitudes [17].

Low-frequency time-dependent voltage fluctuations $u(t)$ across a biased gas sensor, with DC resistance R, can be characterized by their PSD. However the magnitudes of these fluctuations depend on the specific electronic circuit, which is shown in Figure 3a, and therefore we calculated the product $fS_r(f)/R^2$, which corresponds to the PSD of the resistance fluctuations $S_r(f)$ divided by R^2 and multiplied by the frequency f. In this way we achieved better data visualization by highlighting any deviation from $1/f$ noise (flicker noise) [18]. The technique for transforming $u(t)$ into resistance fluctuations was presented elsewhere [19].

The normalized PSD was characteristic for each ambient gas, as shown in Figure 3b. Specifically, the PSD was almost one order of magnitude larger at $f \approx 1$ kHz when formaldehyde vapor was present than in an ambience of pure SA or SA with ethanol. The distribution of the recorded voltage fluctuations—*i.e.*, the number of observations occurring in selected ranges of voltage values, shown in Figure 3c—indicates that random telegraph noise (burst noise exhibiting step-like transitions between a few discrete voltage levels) could be observed only upon exposure to formaldehyde. When pure SA or SA with ethanol were introduced, the noise had a Gaussian probability distribution. The horizontal axis of the distribution presented in Figure 3c displays $\mathrm{sign}(u)\cdot u^2/(2\sigma^2)$, where $\mathrm{sign}(u)$ is the signum function extracting the sign of voltage sample u, and σ is the standard deviation of the recorded voltage fluctuations' time series. This scaling of the horizontal axis, together with exponential scaling of the vertical axis, yields that a

Gaussian distribution is represented by two straight-line segments. Similar noise behaviors were observed during repeated experiments within a period of a few months.

Analogous experiments were performed also at lower bias voltages. In these cases, there were only very small differences among the noise intensities recorded for the various gases; results for U_B = 5 V are depicted in Figure 3d.

The data recorded for the gas sensors may be understood from the existence of an electric field that is high enough to generate random telegraph noise in the organically functionalized AuNPs; this contention is consistent with the explanations for such noise in other materials [20]. We note in passing that the noise detected in the presence of formaldehyde is similar to neural spike trains induced by smell in olfactory cells [21]. The observed signal is strong enough that it does not require additional amplification, and one only needs to sample noise with an A/D converter and estimate its PSD. In fact, it might be possible to apply even simpler analysis methods such as zero-crossing detection with an electronic comparator [22].

When the experiments were repeated using different gases, after eight months, we observed a drift of the gas sensor's characteristic and its sensing ability (Figure 4). Firstly, at the same bias voltage as previously used (U_B = 11.3 V) we observed a train of voltage spikes (as in Figure 3a) even for an ambient atmosphere of SA only. Therefore we decreased U_B to 7 V or 7.5 V by applying a different resistance (660 kΩ; Figure 4a), connected in series with the sensor, than in the previous experiment (Figure 3a). The DC resistance of the biased sensor had changed as well (R = 280 kΩ in SA; R = 318 kΩ when formaldehyde gas was introduced). We suppose that some processes related to AuNP aggregation or migration took place and induced a drift in the sensor's characteristics. Irrespectively of the observed change of its properties, the sensor generated a train of voltage spikes when formaldehyde was introduced into its ambient atmosphere (Figure

4b). The spikes were very intense and were wider than in the previous data (Figure 3a). There was a shift of the maximum of the noise product $fS_r(f)/R^2$ from about $7 \cdot 10^2$ Hz (Figure 3b) to about $1 \cdot 10^2$ Hz (Figure 4c). Similar noise intensities were observed when we introduced formaldehyde diluted in SA at various concentrations, starting from 1.5 ppm and extending up to 10 ppm. When we added ethanol (27 ppm) or further humidity (about 25%), the noise intensity did not change significantly.

The same measurements were repeated during the following days, and we verified that very similar results were obtained. The gas sensor was cleaned by applying a DC voltage of 16 V, of the same polarization as the applied DC bias, for about 45 minutes before starting the repeated measurements.

Effects similar to the ones reported here for functionalized AuNPs were not observed in other previously investigated resistive gas sensors, such as those based on SnO_2 and WO_3 [22, 23] which need elevated operating temperatures to increase the adsorption–desorption processes required for gas sensing. At low operating temperatures, the latter sensing materials behave as semiconductors and intergranular potential barriers are too high to be surmounted by charge carriers.

4. Conclusions

In conclusion, we have reported fluctuation-induced gas sensing measurements for monolayer-capped AuNPs films. Our results suggest that a new type of chemical gas sensor, with limited energy requirement and high gas selectivity, can be developed by recording resistance fluctuations in organically-functionalized AuNPs materials. Proper choice of organic functionality can enhance the sensor's sensitivity toward target VOCs while counteracting its sensitivity for other gases. Therefore, sensors based on AuNPs functionalized with different organic compounds are of much interest for applications in

non-invasive diagnosis through exhaled breath analysis. We envisage that an array of several sensors with different organic ligands could mimic the sense of smell and at the same time be tolerant towards confounding compounds.

We finally note that AuNPs can be prepared by a number of techniques, such as laser ablation/gas deposition [24], sputtering [25] and more. This opens numerous ways towards the practical preparation of gas sensors for biomedical and other applications.

Acknowledgment

This research was partially financed by the National Science Center, Poland, number of the decision: DEC-2012/06/M/ST7/00444 "Detection of gases by means of nanotechnological resistance sensors". R.I. acknowledges a "Ramón y Cajal" fellowship from the Spanish Ministry of Economy and Competiveness (MINECO, Spain) as well as a mobility fellowship from the Catalan Research Agency (AGAUR, Catalonia Region, Spain). U.C. and C.G.G. were supported by the European Research Council under the European Community's Seventh Framework Program (FP/2007–2013)/ERC Grant Agreement No. 267234 (GRINDOOR).

Author Contributions

The manuscript was written through contributions of all authors. All authors have given approval to the final version of the manuscript.

Supplementary material

Material characterisation techniques and micro-processing of gas sensing devices.

References

[1] M. Hakim, Y.Y. Broza, O. Barash, N. Peled, M. Phillips, A. Amann, H. Haick, Volatile organic compounds of lung cancer and possible biochemical pathways, Chem. Rev. 112 (2012) 5949–5966.

[2] P. Mazzone, Progress in the development of a diagnostic test for lung cancer through the analysis of breath volatiles, J. Breath Res. 2 (2008) 037014.

[3] G. Peng, U. Tisch, O. Adams, M. Hakim, N. Shehada, Y.Y. Broza, S. Billan, R. Abdah-Bortnyak, A. Kuten, H. Haick, Diagnosing lung cancer in exhaled breath using gold nanoparticles, Nat. Nanotechnol. 4 (2009) 669–73.

[4] P. Fuchs, C. Loeseken, J.K. Schubert, W. Miekisch, Breath gas aldehydes as biomarkers of lung cancer, Int. J. Cancer 126 (2010) 2663–2670.

[5] P. Španěl, D. Smith, Quantification of trace levels of the potential cancer biomarkers formaldehyde, acetaldehyde and propanol in breath by SIFT-MS, J. Breath Res. 2 (2008) 046003.

[6] M.K. Nakhleh, Y.Y. Broza, H. Haick, Monolayer-capped gold nanoparticles for disease detection from breath, Nanomedicine 9 (2014) 1991–2002.

[7] E. Ozawa, Y. Kawakami, T. Seto, T. Formation and size control of tungsten nanoparticles produced by Nd: YAG laser irradiation, Scr. Mater. 44 (2001) 2279–2283.

[8] D. Buso, M. Post, C. Cantalini, P. Mulvaney, A. Martucci, Gold nanoparticle-doped TiO_2 semiconductor thin films: Gas sensing properties, Adv. Funct. Mater. 18 (2008) 3843–3849.

[9] S. Vallejos, T. Stoycheva, P. Umek, C. Navio, R. Snyders, C. Bittencourt, E. Llobet, Ch. Blackman, S. Moniz, X. Correig, Au nanoparticle-functionalised WO_3

nanoneedles and their application in high sensitivity gas sensor devices, Chem. Commun. 47 (2011) 565–567.

[10] P. Weisz, Effects of electronic charge transfer between adsorbate and solid on chemisorption and catalysis, J. Chem. Phys. 21 (1953) 1531–1538.

[11] L. Kish, R. Vajtai, C. Granqvist, Extracting information from noise spectra of chemical sensors: single sensor electronic noses and tongues, Sens. Actuators B 71 (2000) 55–59.

[12] M.M. Kotarski, J.M. Smulko, Hazardous gases detection by fluctuation-enhanced gas sensing, Fluct. Noise Lett. 9 (2010) 359–371.

[13] J. Ederth, J. Smulko, L.B. Kish, P. Heszler, C.G. Granqvist, Comparison of classical and fluctuation-enhanced gas sensing with Pd_xWO_3 nanoparticle films, Sens. Actuators B 113 (2006) 310–315.

[14] M. Brust, J. Fink, D. Bethell, D. Schiffrin, C. Kiely, Synthesis and reactions of functionalised gold nanoparticles, J. Chem. Soc., Chem. Commun. 16 (1995) 1655–1656.

[15] J. Guo, P. Pang, Q. Cai, Effect of trace residual ionic impurities on the response of chemiresistor sensors with dithiol-linked monolayer-protected gold (nano) clusters as sensing interfaces, Sens. Actuators B 120 (2007) 521–528.

[16] C. Granqvist, R. Buhrman, Ultrafine metal particles, J. Appl. Phys. 47 (1976) 2200–2219.

[17] J.S. Bendat, A.G. Piersol, Random data: analysis and measurement procedures, John Wiley & Sons, 2011.

[18] J. Solis, L. Kish, R. Vajtai, C. Granqvist, J. Olsson, J. Schnürer, V. Lantto, Identifying natural and artificial odours through noise analysis with a sampling-and-hold electronic nose, Sens. Actuators B 77 (2001) 312–315.

[19] B. Ayhan, C. Kwan, J. Zhou, L.B. Kish, K.D. Benkstein, P.H. Rogers, S. Semancik, Fluctuation enhanced sensing (FES) with a nanostructured, semiconducting metal oxide film for gas detection and classification, Sens. Actuators B 188 (2013) 651–660.

[20] K.K. Hung, H. Chenming, Y.C. Cheng, Random telegraph noise of deep-submicrometer MOSFETs, IEEE Electron. Device Lett. 11 (1990) 90–92.

[21] T. Otto, H. Eichenbaum, C.G. Wible, S.I. Wiener, Learning-related patterns of CA1 spike trains parallel stimulation parameters optimal for inducing hippocampal long-term potentiation, Hippocampus 1 (1991) 181–192.

[22] Ł. Lentka, J.M. Smulko, R. Ionescu, C.G. Granqvist, L.B Kish, Determination of gas. mixture components using fluctuation enhanced sensing and the LS-SVM regression algorithm, Metrol. Meas. Syst. 22 (2015) 341–350.

[23] R. Macku, J. Smulko, P. Koktavy, M. Trawka, P. Sedlak, Analytical fluctuation enhanced sensing by resistive gas sensors, Sens. Actuators B 213 (2015) 390–396.

[24] Y. Kawakami, T. Seto, T. Yoshida, E. Ozawa, Gold nanoparticles and films produced by a laser ablation/gas deposition (LAGD) method, Appl. Surf. Sci. 197 (2002) 587–593.

[25] O. Kvitek, R. Hendrych, Z. Kolska, V. Svorcik, Grafting of gold nanoparticles on glass using sputtered gold interlayers, J. Chem. 258 (2012) 8991–8995.

Captions to the figures

Figure 1. (a) Schematic representation of the AGD equipment used for ultra-pure AuNP synthesis. (b) SEM image (top view) of a layer of AuNPs functionalized with 2-mercaptobenzoxazole. (c) XPS spectrum for a layer of functionalized AuNPs.

Figure 2. Current–voltage (*I–U*) characteristic of the investigated gas sensor operated at room temperature (22°C) in synthetic dry air.

Figure 3. (a) Time-dependent voltage fluctuations $u(t)$ across a gas sensor of resistance R upon its exposure to formaldehyde vapor at a bias voltage U_B of 11.3 V; the sensor was connected in series with a resistance of 390 kΩ as shown in the circuit diagram. (b) Power spectral density $S_r(f)$ of the sensor's resistance fluctuations, multiplied by frequency f and divided by the square of the sensor's DC resistance (246 kΩ), upon exposure to the shown gases at a bias voltage U_B of 11.3 V. (c) Distribution of voltage fluctuations, with standard deviation σ, across the sensor upon its exposure to the shown gases at a bias voltage U_B of 11.3 V (also see the main text). (d) Power spectral density $S_r(f)$ of the sensor's resistance fluctuations, multiplied by frequency f and divided by the square of the sensor's DC resistance (526 kΩ), upon exposure to the shown gases at a bias voltage U_B of 5 V.

Figure 4. (a) Time-dependent voltage fluctuations $u(t)$ across a gas sensor of resistance R = 280 kΩ upon its exposure to synthetic air at a bias voltage U_B of 7.5 V; the sensor was connected in series with a resistance of 660 kΩ as shown in the circuit diagram. (b) Time-dependent voltage fluctuations across a gas sensor of resistance R = 318 kΩ upon

its exposure to formaldehyde 10 ppm diluted in synthetic air at U_B = 7 V; the sensor was connected in series with a resistance of 660 kΩ. (c) Power spectral density $S_r(f)$ of the sensor's resistance fluctuations, multiplied by frequency f and divided by the square of the sensor's DC resistance, upon exposure to the shown gases at U_B = 7.5 V (synthetic air) or U_B = 7 V (all others reported gas mixtures).

(a)

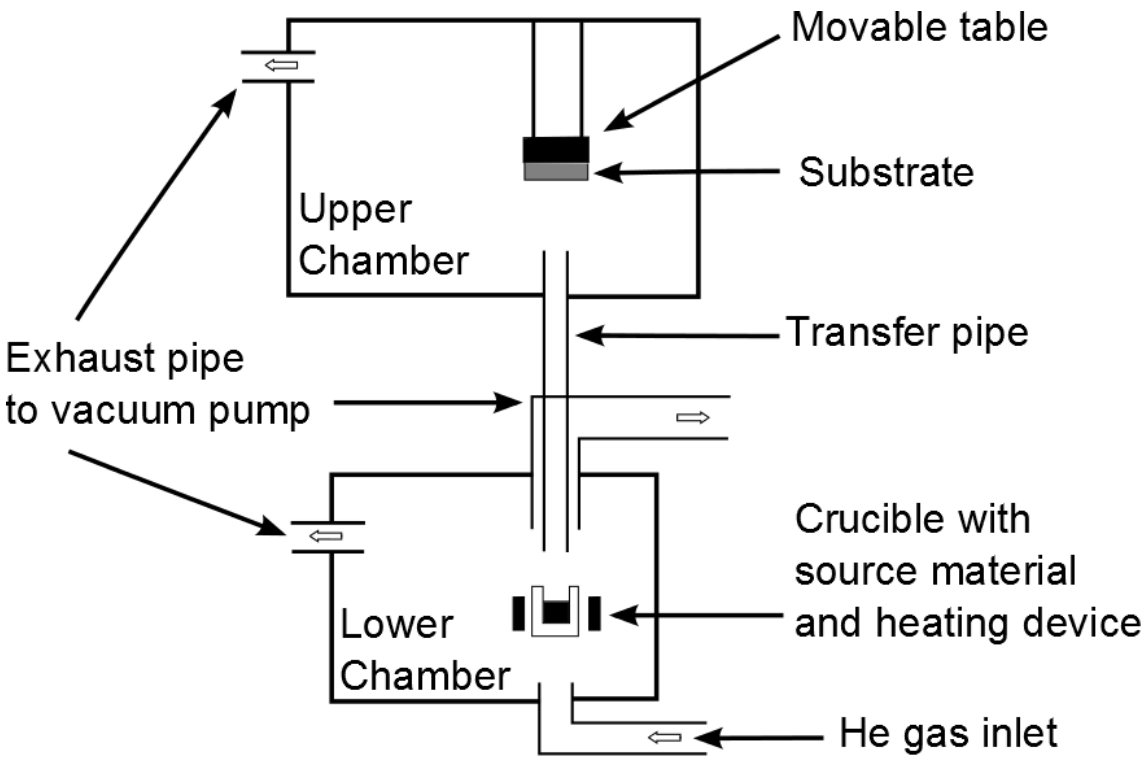

(b)

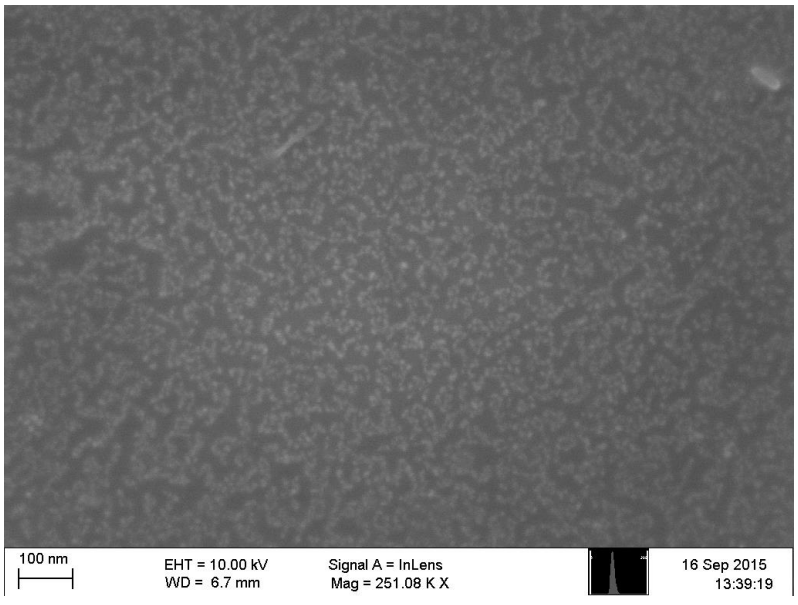

(c)

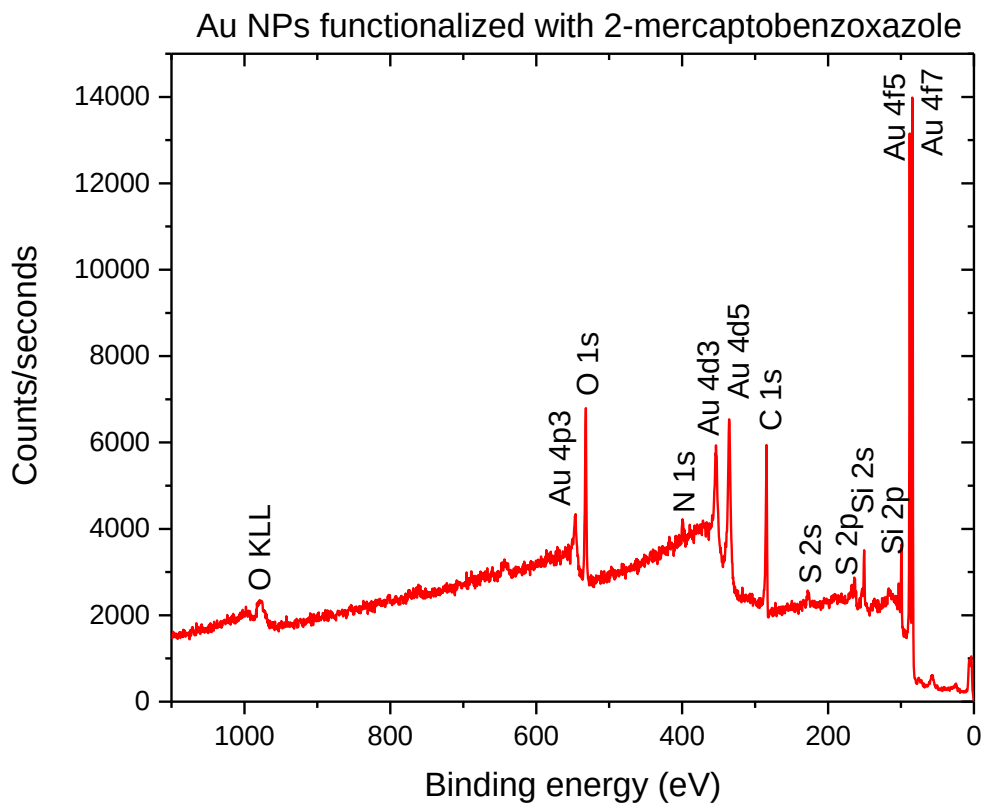

Figure 1

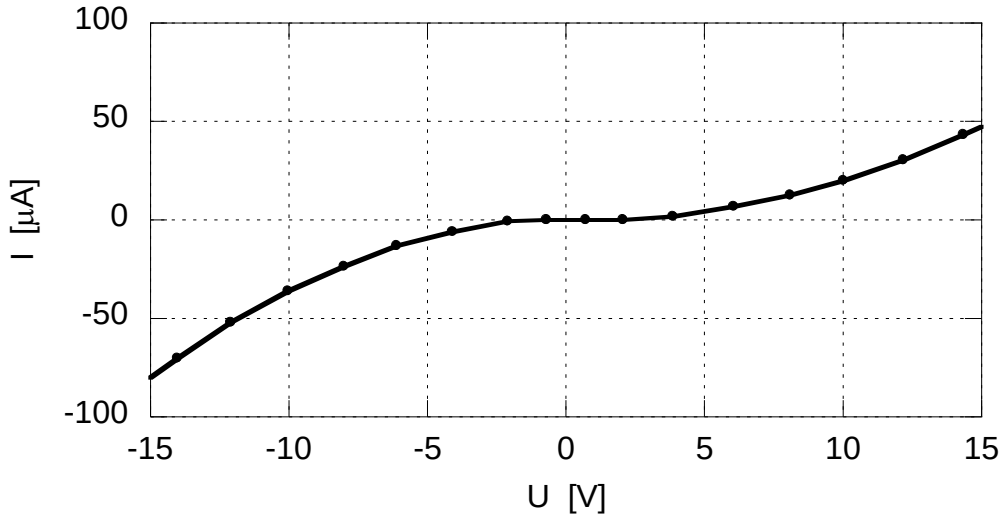

Figure 2

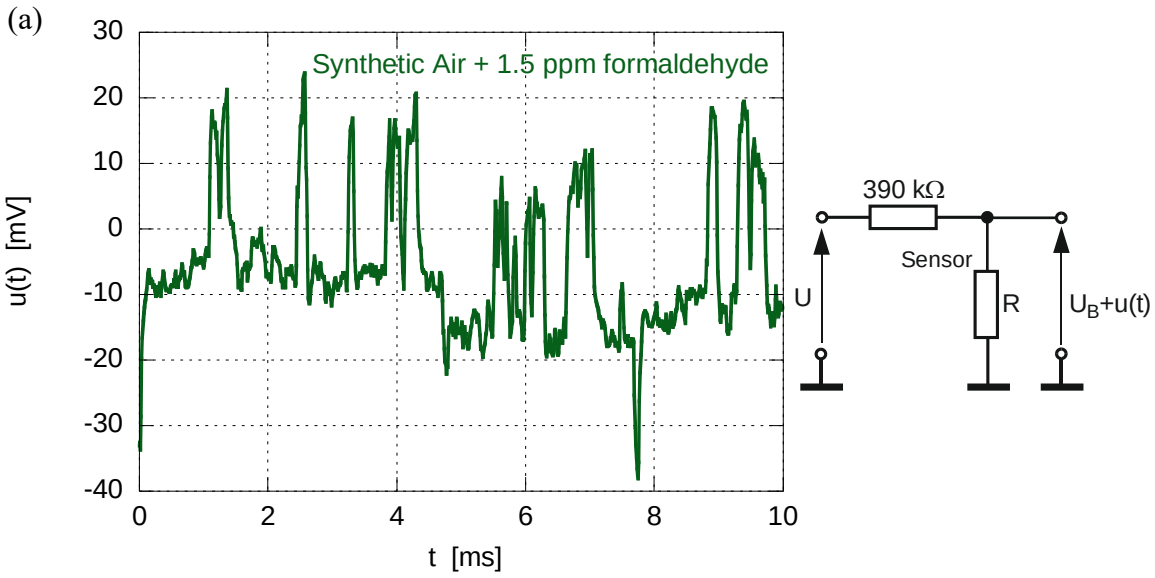

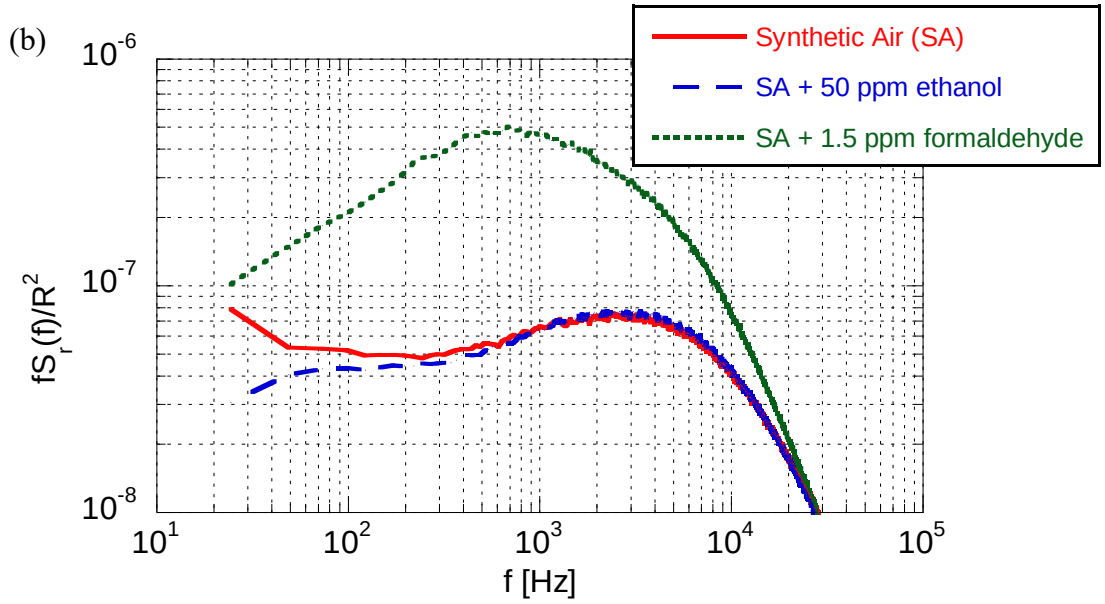

(c)

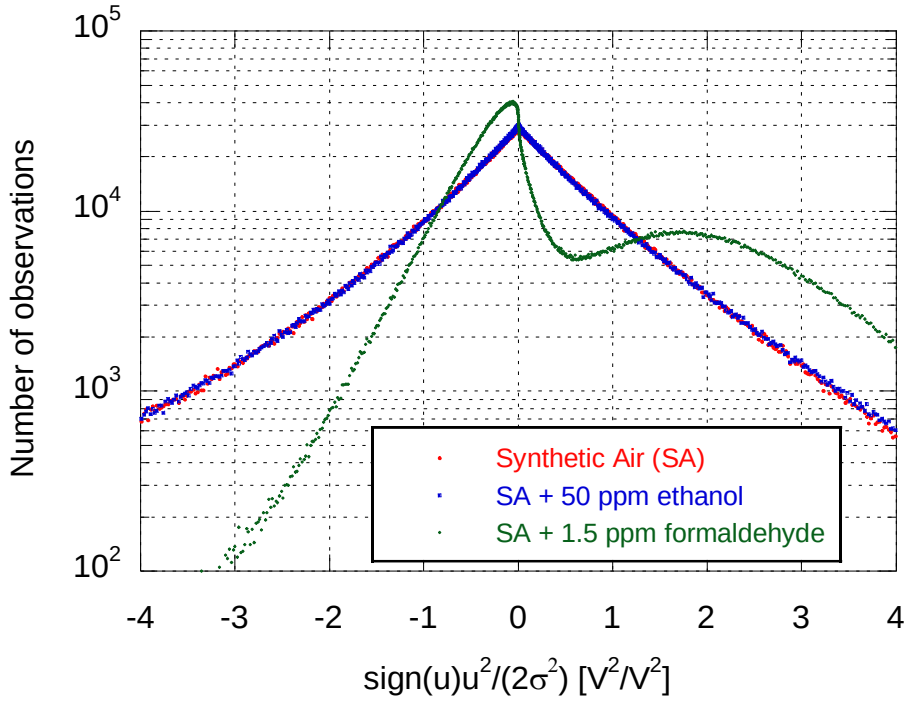

(d)

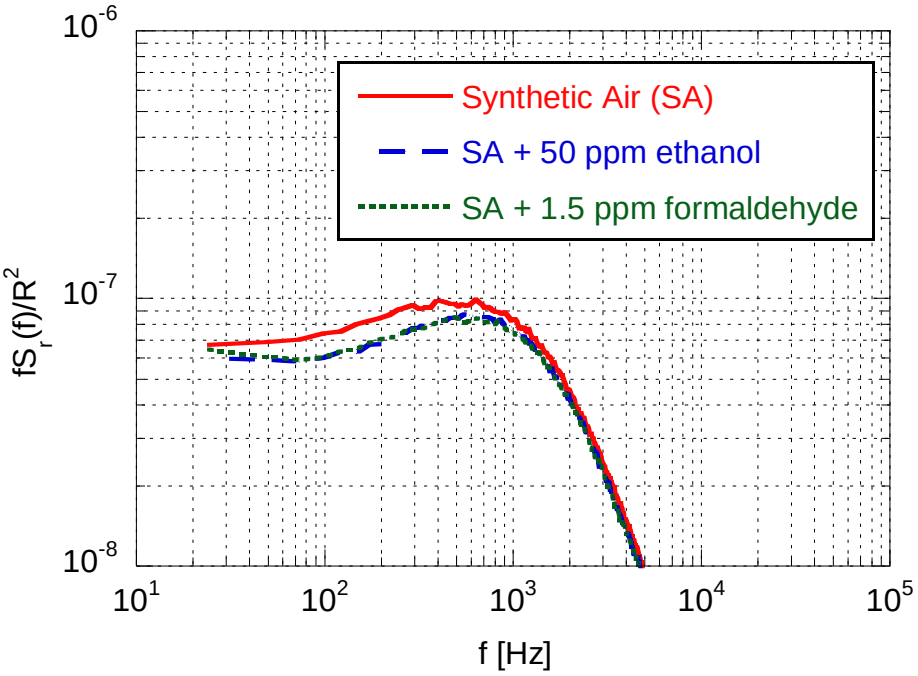

Figure 3

(a)

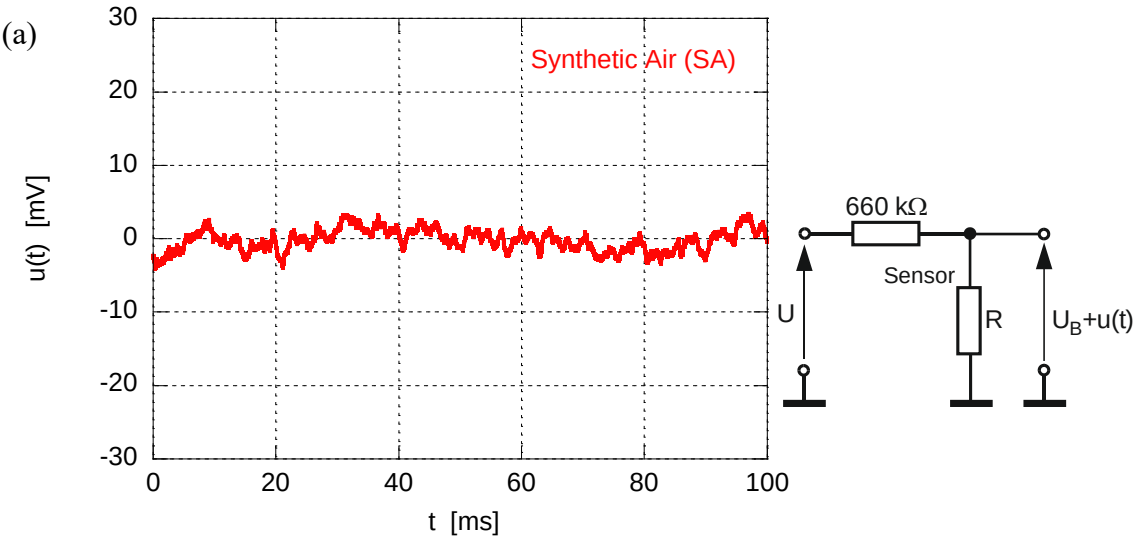

(b)

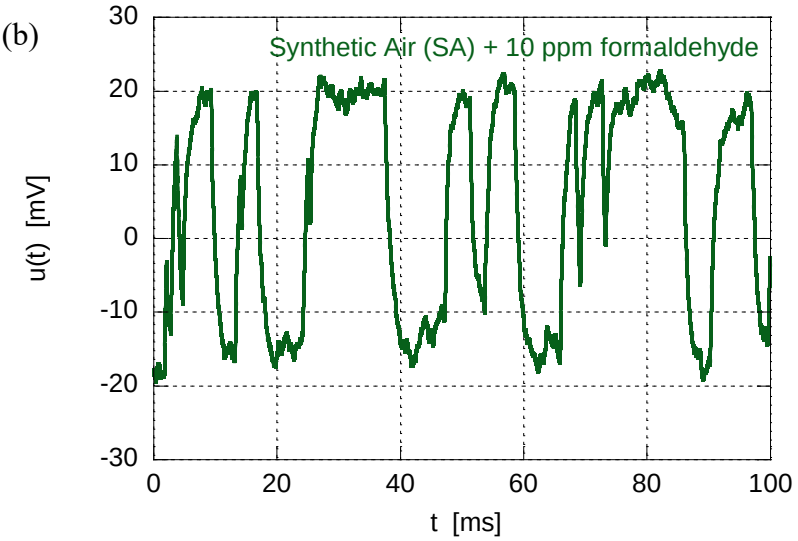

(c)

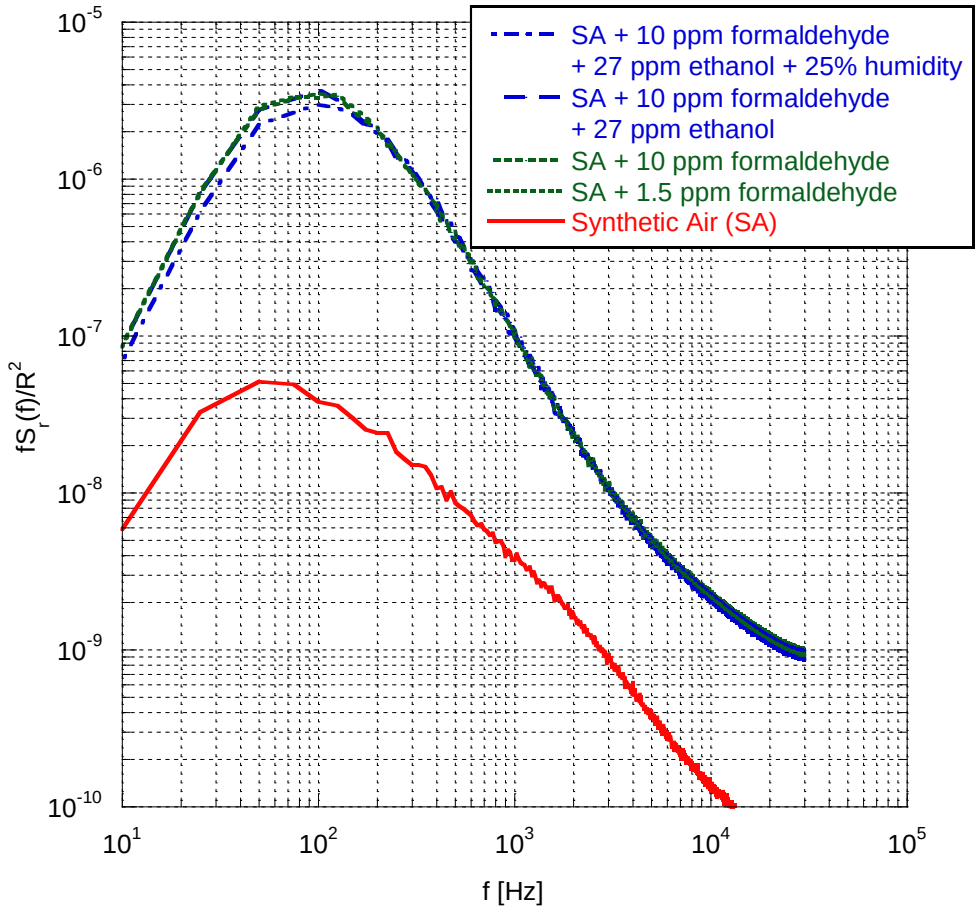

Figure 4